Supporting Information for

Serotonin is the Common Thread Linking Different Classes of Antidepressants

Colby E. Witt, Sergio Mena, Jordan Holmes, Melinda Hersey, Anna Marie Buchanan, Brenna Parke, Rachel Saylor, Lauren E. Honan, Shane N. Berger, Sara Lumbreras, Frederik H. Nijhout, Michael C. Reed, Janet Best, James Fadel, Patrick Schloss, Thorsten Lau, and Parastoo Hashemi

Corresponding author: Parastoo Hashemi
Email: p.hashemi04@imperial.ac.uk

This PDF file includes:

Supplementary extended results section
Figures S1 and S2

Supporting Information

Extended Results

How Do Antidepressants with Different Modes of Action Affect Ambient Extracellular Serotonin?

Figure 1A shows the experimental paradigm for serotonin voltammetry. Briefly, animals were anesthetized, underwent stereotaxic surgery whereby a stimulating electrode was placed in the medial forebrain bundle (MFB) and a carbon fiber microelectrode (CFM) was placed in the CA2 region of the hippocampus. FSCV was used to isolate an area where an electrically evoked serotonin signal was present (a 30 second file showing the release and reuptake profile for serotonin). The experimental mode was then switched to FSCAV to acquire minute-to-minute basal level measurements. After a 30-minute period of control files, 5 mL kg^{-1} saline was given intraperitoneally (i.p.), and 30 minutes after that, a drug was given (i.p.). After 60 minutes of drug files were collected, the experimental mode was switched back to FSCV to assess the effect of the drug on evoked release and reuptake.

Figure 1B shows representative FSCV and FSCAV color plots, cyclic voltammograms (CV) and current *vs.* time (IT) (for FSCV). The black space in the FSCAV color plot indicates the holding period. **Figure 1C** shows the ambient serotonin levels after drug challenge with escitalopram, fluoxetine, reboxetine and ketamine. Each trace is an average of 5 animals ± the SEM (error bars). **Figure 1D** shows the structure and mode of action of each of these agents. A repeated measures analysis of variance (ANOVA) and analysis of covariance (ANCOVA) with post-hoc comparisons were used to analyze time point and slope changes in extracellular concentrations of serotonin. Saline administration did not have a significant effect with respect to the control state prior to escitalopram (post-hoc paired *t*-test, 34.91 ± 1.03 nM *vs.* 31.50 ± 1.41 nM, p = 0.2838; slope *t*-test, 0.08 ± 0.01 nM min^{-1} vs. -0.10 ± 0.01 nM min^{-1}, p = 0.1307), fluoxetine (post-hoc paired *t*-test, 40.90 ± 1.87 nM *vs.* 42.47 ± 1.85 nM, p = 0.2620; slope *t*-test, -0.06 ± 0.01 nM min^{-1} vs. 0.12 ± 0.01 nM min^{-1}, p = 0.9770), reboxetine (post-hoc paired *t*-test, 40.33 ± 1.32 nM *vs.* 42.42 ± 1.45 nM, p = 0.5379; slope *t*-test, 0.12 ± 0.01 nM min^{-1} vs. 0.18 ± 0.01 nM min^{-1}, p = 0.7377) and ketamine (post-hoc paired *t*-test, 28.48 ± 0.77 nM *vs.* 23.81 ± 1.24 nM, p = 0.1968; slope *t*-test, -0.09 ± 0.01 nM min^{-1} vs. -0.03 ± 0.01 nM min^{-1}, p = 0.9880). Sixty minutes after drug administration, escitalopram significantly increases serotonin from 34.91 ± 1.03 nM to 54.59 ± 14.76 nM (post-hoc paired *t*-test, p = 0.0314; slope *t*-test, 0.08 ± 0.01 nM min^{-1} vs. 0.60 ± 0.00 nM min^{-1}, p = 0.0022), fluoxetine from 40.90 ± 1.87 nM to 62.71 ± 20.80 nM (post-hoc paired *t*-test, p = 0.0167; slope *t*-test, -0.06 ± 0.01 nM min^{-1} vs. 0.36 ± 0.00 nM min^{-1}, p = 0.0015), reboxetine from 40.33 ± 1.32 nM to 72.48 ± 14.22 nM (post-hoc paired *t*-test, p = 0.0104; slope *t*-test, 0.12 ± 0.01 nM min^{-1} vs. 0.48 ± 0.00 nM min^{-1}, p = 0.0165) and ketamine from 28.48 ± 0.77 nM to 39.59 ± 5.59 nM (post-hoc paired *t*-test, p = 0.1872; slope *t*-test, -0.09 ± 0.01 nM min^{-1} vs. 0.28 ± 0.00 nM min^{-1}, p = 0.0001). The fastest rate of increase of serotonin concentration was found to be after escitalopram administration, which was significantly higher than fluoxetine and ketamine, but not reboxetine (slope *t*-tests, 0.60 ± 0.00 nM min^{-1} vs. 0.36 ± 0.00 nM min^{-1}, p < 0.0001; 0.60 ± 0.00 nM min^{-1} vs. 0.28 ± 0.00 nM min^{-1}, p < 0.0001; 0.60 ± 0.00 nM min^{-1} vs. 0.36 ± 0.00 nM min^{-1}, p = 0.1741).

Serotonin Reuptake Kinetics Between Different Antidepressants

In prior work we discovered that extracellular serotonin concentrations oscillate in the hippocampus around a mean with a period of approximately 5-7 minutes(1). Using power spectrum density (PSD) analysis, we found that the frequency spectra of these oscillations did not differ in male and female

mice, nor did they differ in mice that had undergone a chronic stress paradigm *vs.* their age-matched controls. We found differences in frequency when we administered SSRIs. Specifically, we found that after escitalopram administration, the frequency of oscillation increased. Here we repeat this PSD analysis in a set of experiments with the 4 antidepressants above. **Figure 2A(i)** shows a representative example of the filtered FSCAV data collected for 60 minutes before (black) and 60 minutes after fluoxetine (blue), **Fig. 2A(ii)** is the mean and SEM (n = 5 mice) normalized PSD before drug (black) and after drug (blue), **Fig. 2A(iii)** is a violin plot showing the distribution of the sum of power-weighted frequencies (WF) from the power spectra. **Figure. 2B, C** and **D** show the same data and analysis for escitalopram (green), reboxetine (red) and ketamine (purple). Using the sum of power-weighted frequencies (a measure of displacement of the whole power spectra, see Methods section), we found the weighted frequencies increased after administration of fluoxetine (paired t-test, WF = 0.45 ± 0.03 p.d.u. vs. WF = 0.51 ± 0.03 p.d.u. , p = 0.0907) and escitalopram (paired t-test, WF = 0.28 ± 0.01 p.d.u. vs. WF = 0.34 ± 0.02 p.d.u., p = 0.0285) (suggesting Uptake 1 inhibition), decreased after administration of reboxetine (implying Uptake 2 inhibition) (paired t-test, WF = 0.40 ± 0.03 p.d.u. vs. WF = 0.32 ± 0.03 p.d.u., p = 0.0393) and did not change after ketamine administration (paired t-test, WF = 0.44 ± 0.05 p.d.u. vs. WF = 0.43 ± 0.05 p.d.u., p = 0.8875) (showing no change in reuptake).

To further test how these agents changed the profile of serotonin reuptake we performed FSCV analysis of evoked serotonin. In **Fig. 2(iv)** we show control (black) and 60 minutes after drug (color) stimulated hippocampal serotonin release. We found that the maximum amplitude of release and clearance rate significantly increased 60 min after administration of fluoxetine (paired *t*-test, Amp_{max} = 35.37 ± 5.61 nM vs. Amp_{max} = 57.03 ± 11.28 nM, p = 0.0063) (paired *t*-test, $t_{1/2}$ = 2.13 ± 0.30 s vs. $t_{1/2}$ = 5.30 ± 0.88 s, p = 0.0197), escitalopram (paired *t*-test, Amp_{max} = 24.61 ± 6.29 nM vs. Amp_{max} = 42.63 ± 13.06 nM, p = 0.0467) (paired *t*-test, $t_{1/2}$ = 1.87 ± 0.28 s vs. $t_{1/2}$ = 49.07 ± 19.91 s, p = 0.0446) and reboxetine (paired *t*-test, Amp_{max} = 44.82 ± 17.17 nM vs. Amp_{max} = 57.37 ± 21.10 nM, p = 0.0417) (paired *t*-test, $t_{1/2}$ = 2.33 ± 0.26 s vs. $t_{1/2}$ = 10.70 ± 1.25 s, p = 0.0030), but not ketamine (paired *t*-test, Amp_{max} = 32.29 ± 10.89 nM vs. Amp_{max} = 32.18 ± 10.28 nM, p = 0.9903) (paired *t*-test, $t_{1/2}$ = 1.44 ± 0.16 s vs. $t_{1/2}$ = 2.69 ± 0.60 s, p = 0.1098).

Next, we fit these responses with the M-M model of dual reuptake (Uptake 1 and 2) shown in Equation 1:

$$dC(t)/dt = R(t)(1 - A(t)) - \alpha \frac{V_{max1} \cdot C(t)}{K_{m1} + C(t)} - \beta \frac{V_{max2} \cdot C(t)}{K_{m2} + C(t)} \quad (1)$$

Where *C(t)*, *R(t)* and *A(t)* represent the concentration of the neurotransmitter, evoked release rate and autoreceptor control at time t, respectively. V_{max} and K_m are M-M parameters and α and β are the rates of Uptake 1 and Uptake 2. In this model, Uptake 1 represents a high-affinity, low-capacity system (serotonin transporters (SERTs)) and Uptake 2 is a low-affinity, high-capacity system (norepinephrine, dopamine, organic cation transporters and plasma membrane monoamine transporters (NETs, DATs and OCTs and PMATs)). The results of the modeling (shown as ratio of change with respect to control) are in the table in **Fig. 2E**. **Figure 2F** is a synthesized response where hypothetical scenarios are modeled. These scenarios are Uptake 2 inhibition *via* K_{m2} (blue), Uptake 1 inhibition *via* K_{m1} (orange) and Uptake 1 inhibition (*via* change in both K_{m1} and V_{max1}; red). SERT inhibition with fluoxetine follows a typical orthosteric inhibition profile, where a change in K_{m1} (orange curve in **Fig. 2F**) can easily fit the curve. Uptake inhibition with reboxetine follows mainly Uptake 2 inhibition, where the curve can be modeled by primarily a change in K_{m2} (resembling the blue trace in **Fig. 2F**). Ketamine does not change the kinetics of the curve. Escitalopram is the most unusual response in that it cannot be fit with a change in K_{m1} (consistent with SERT inhibition). Here we also needed to substantially alter V_{max1} to fit the curve (red curve in **Fig. 2F**). Competitive uptake inhibition should not ordinarily change V_{max} therefore we found it interesting to study escitalopram more thoroughly *via* detailed dose response experiments.

A Temporo-Dose Response for Escitalopram

To evaluate the effects of different doses of escitalopram on serotonin, we administered 4 different doses to cohorts of mice and performed a time after drug analysis for each dose (1-30 mg kg^{-1} in **Fig. 3A-D(i)**). The data is from female mice, however male mice respond similarly and are shown in the supplementary information (**Fig. S1**). The control (before drug) response is shown in black for all doses and then shown 5, 30, 60, 90 and 120 minutes after escitalopram. **Figure 3E** depicts our pharmacokinetic model, the four-compartment model (FCM), used to obtain an estimation of escitalopram concentration in the brain of a mouse. In this model, we simulate the physiological path of an acute *i.p.* injection of escitalopram, from 4 different compartments in the body with different concentrations of the drug: the peritoneum ($C_0(t)$), plasma ($C_1(t)$), brain extracellular space ($C_2(t)$) and periphery ($C_3(t)$). The arrows of the model depict interchange of escitalopram between compartments. The rate constants, k, determine the speed of escitalopram interchange (nM min^{-1}) from one compartment to another, or to secretion (k_{10}). The model considers the partial bioavailability of the drug after peritoneal injection, the percentage of protein binding (*e.g.,* albumin) to the drug in plasma and the retention of escitalopram in the brain due to binding to SERTs. Solving the system of equations provides concentration vs. time traces for escitalopram for each body compartment. For this work, we were interested in escitalopram concentration in the extracellular hippocampal space. Full description of the parameters of the model can be found in the Methods section.

Figure 3A-D(ii) are the results of the theoretical temporo-dose response where K_{m1} is altered as per theoretical uptake inhibition(2) of SERTs from escitalopram, while the rest of the release and uptake parameters are kept constant with respect to control. In these theoretical curves, as the dose increases, both maximum amplitude and $t_{1/2}$ of reuptake also increase. In terms of the temporal response, for the 1 mg kg^{-1} dose and 5 minutes after drug the response is not meaningfully different from control, and the 30-, 60-, 90- and 120-minute responses are not substantially different from each other, since the modeled concentration of escitalopram (**Fig. 3E**) does not substantially change. For the 3 mg kg^{-1} dose, this behavior is repeated. For the 10 and 30 mg kg^{-1} doses, the 5 minute responses are not different from the later time points due to higher doses increasing escitalopram in the brain more rapidly. **Figure 3F-H** shows the ratio changes of maximum release, K_{m1} and V_{max1}. In **Fig. 3F**, the ratio of release amplitude does not substantially change with time for the 1 mg kg^{-1} dose (e.g., 60 min after injection, $R(t)_{max}$ = 46.40 nM s^{-1}, 1.01 ratio *vs.* control). For all other doses it falls with time (3 mg kg^{-1}: $R(t)_{max}$ = 42.00 nM s^{-1}, ratio of 0.92 *vs.* control; 10 mg kg^{-1}: $R(t)_{max}$ = 30.80 nM s^{-1}, ratio of 0.76 *vs.* control; 30 mg kg^{-1}: $R(t)_{max}$ = 33.00 nM s^{-1}, ratio of 0.73 *vs.* control). For all doses, the K_{m1} increases with time. A finding of interest is that while at 1 mg kg^{-1} after 5 minutes the K_{m1} increases (K_{m1} = 13.03 nM, ratio of 6.52 *vs.* control), for 3 mg kg^{-1} at 5 minutes K_{m1} does not increase (inset) (K_{m1} = 2.50 nM, ratio of 0.96 *vs.* control). In general, V_{max1} decreases with time for all doses. A finding of interest here is that for 3 and 10 mg kg^{-1}, V_{max1} increases 5 min after drug administration (3 mg kg^{-1}: V_{max1} = 12.02 nM s^{-1}, ratio of 1.12 *vs.* control; 10 mg kg^{-1}: V_{max1} = 14.32 nM s^{-1}, ratio of 1.13 *vs.* control). **Figure 3I** is a comparison of the effects on the basal serotonin levels in separate cohorts of mice for 1, 3 and 10 mg kg^{-1}. We chose to compare these three doses to gather more information on the similarity between K_{m1} of the 3 and 10 mg kg^{-1} doses. After a control period of 30 minutes, a 5 mL kg^{-1} saline *i.p.* injection was given, and files were collected for another 30 minutes. After this, the drug was given and the serotonin levels were measured for a further 60 minutes. Saline did not have a significant impact on the measured extracellular levels of serotonin prior to a dose of 1 mg

kg^{-1} (post-hoc paired *t*-test, 33.46 ± 0.93 nM *vs.* 34.73 ± 1.18 nM, p = 0.6524; slope *t*-test, -0.03 ± 0.01 nM min^{-1} vs. -0.00 ± 0.01 nM min^{-1}, p =1.000), 3 mg kg^{-1} (post-hoc paired *t*-test, 29.30 ± 1.33 nM *vs.* 28.35 ± 1.12 nM, p =0.6371; slope *t*-test, -0.08 ± 0.01 nM min^{-1} vs. 0.03 ± 0.01 nM min^{-1}, p =0.9652) and 10 mg kg^{-1} (post-hoc paired *t*-test, 34.91 ± 1.03 nM *vs.* 31.50 ± 1.41 nM, p = 0.2838; slope *t*-test, 0.08 ± 0.01 nM min^{-1} vs. -0.10 ± 0.01 nM min^{-1}, p = 0.1307). At the end of this period, serotonin increased from 33.46 ± 0.93 nM to 44.44 ± 5.99 nM when animals were given a 1 mg kg^{-1} dose (post-hoc paired *t*-test, p =0.0287; slope *t*-test, -0.03 ± 0.01 nM min^{-1} vs.0.19 ± 0.00 nM min^{-1}, p =0.0457), from 29.30 ± 1.33 nM to 31.08 ± 8.66 nM when given 3 mg kg^{-1} (post-hoc paired *t*-test, p = 0.9655; slope *t*-test, -0.08 ± 0.01 nM min^{-1} vs. 0.06 ± 0.00 nM min^{-1}, p = 0.5192) and from 34.91 ± 1.03 nM to 54.59 ± 14.76 nM when given 10 mg kg^{-1} (post-hoc paired *t*-test, p = 0.0314; slope *t*-test, 0.08 ± 0.01 nM min^{-1} vs. 0.60 ± 0.00 nM min^{-1}, p = 0.0022).

The fastest rate of increase of extracellular serotonin was found to be after administration of a dose of 10 mg kg^{-1}, which was significantly higher than after a dose of 3 mg kg^{-1} (slope *t*-test, 0.60 ± 0.00 nM min^{-1} *vs.* 0.06 ± 0.00 nM min^{-1}, p < 0.0001) and 1 mg kg^{-1} (slope *t*-test, 0.60 ± 0.00 nM min^{-1} *vs.* 0.19 ± 0.00 nM min^{-1}, p < 0.0001). An interesting finding is the higher rate of increase of serotonin after a dose of 1 mg kg^{-1} *vs.* 3 mg kg^{-1} (slope *t*-test, 0.19 ± 0.00 nM min^{-1} *vs.* 0.06 ± 0.00 nM min^{-1}, p = 0.0073).

To delve further into the unusual K_{m1} and V_{max1} profile at 5 minutes after escitalopram for the 3 and 10 mg kg^{-1} doses, we studied SERT expression and activity in a cellular model.

SERT Expression/Function in Cellular Model of In Vivo-like Serotonergic Transmission

We studied SERT expression and function in a mouse model of serotonergic transmission. **Figure 4A** shows immunofluorescence of cell surface-located SERTs(3, 4). **Figure 4B** are representative regions of interest where SERTs were quantified at rest, 2 minutes after potassium (K^+) stimulation, 1 µM escitalopram, and with both K^+ and escitalopram. **Figure 4C** shows that escitalopram caused significant reductions in SERT expression after 2 and 5 minutes with respect to control, as seen previously for longer SSRI exposure (> 2 hrs)(22) (Dunn's tests, 2 min: 32.80 ± 0.45 a.u./μM^2 vs. 29.67 ± 0.32 a.u./μM^2, p < 0.0001; 5 min: 32.80 ± 0.45 a.u./μM^2 vs. 29.19 ± 0.22 a.u./μM^2, p < 0.0001). K^+ stimulation caused an increase in SERT expression after 2 and 5 minutes (significant at 5 minutes). (Dunn's tests, 2 min: 32.80 ± 0.45 a.u./μM^2 vs. 34.88 ± 0.47 a.u./μM^2, p = 0.1809; 5 min: 32.80 ± 0.45 a.u./μM^2 vs. 35.01 ± 0.31 a.u./μM^2, p = 0.04946). These data show that K^+ stimulation and a combination of K^+ stimulation and escitalopram increase surface SERT density.

Figure 4D shows that the fluorescent SERT substrate ASP^+ is taken up by the cells and localized to neurites and cell bodies. **Figure 4E** shows example regions of interest used for quantification of SERT uptake at rest, with electrical stimulation, 2 minutes after 1 µM escitalopram, and with electrical stimulation and escitalopram. **Figure 4F** shows that ASP^+ uptake diminished 2 minutes and 5 minutes after escitalopram (significant) (Dunn's tests, 2 min: 30.54 ± 0.31 a.u./μM^2 vs. 27.95 ± 0.38 a.u./μM^2, p = 0.0219; 5 min: 30.46 ± 0.62 a.u./μM^2 vs. 35.42 ± 0.25 a.u./μM^2, p < 0.0001). Electrical stimulation increased ASP^+ uptake after 2 minutes (near significant) (Dunn's tests, 2 min: 30.54 ± 0.31 a.u./μM^2 vs. 32.91 ± 0.45 a.u./μM^2, p = 0.0559; 5 min: 30.46 ± 0.62 a.u./μM^2 vs. 32.19 ± 0.29 a.u./μM^2, p = 0.3792). These data show that, in synergy with increasing SERT density, electrical stimulation and escitalopram increase SERT activity.

As proof of principle that the increased SERT expression/activity in response to the 2 stimulations (K^+ and electrical) is mediated by serotonin, we next showed that an acute application of only serotonin (0.1 µM and 1 µM) resulted in increased ASP^+ uptake after 2 minutes and 5 minutes (**Fig. 4G**) (Dunn's tests for 2 min, 0.1 µM: 100.26 ± 1.17% vs. 102.64 ± 1.21%, p = 0.1301; 1 µM: 100.26 ± 1.17% vs. 105.58 ± 0.63%, p < 0.0001) (Dunn's tests for 5 min, 0.1 µM: 100.86 ± 0.47% vs. 103.88± 0.77%, p = 0.0137; 1 µM: 100.86 ± 0.47% vs. 109.20 ± 0.98%, p < 0.0001). Adding escitalopram to the excess serotonin model was not able to reverse the increase in ASP^+ uptake. (Dunn's tests for 2 min, 0.1 µM: 96.04 ± 0.55% vs. 103.35 ± 1.03%, p < 0.0001; 1 µM: 96.04 ± 0.55% vs. 104.47 ± 0.86%, p < 0.0001) (Dunn's tests for 5 min, 0.1 µM: 92.65 ± 0.96% vs. 102.49 ± 0.80%, p < 0.0001; 1 µM: 92.65 ± 0.96% vs. 107.58 ± 0.78%, p < 0.0001). This increased reuptake behavior does not extend to another SSRI, fluoxetine. **Figure 4H** is a comparison of ASP^+ uptake in the presence of 1 µM escitalopram or 10 µM fluoxetine with the cells at rest or 5 minutes after electrical stimulation. Without stimulation, fluoxetine did not significantly affect ASP^+ uptake (Dunn's test, 61.82 ± 0.70 a.u./μM^2 vs. 60.24 ± 0.62 a.u./μM^2, p = 0.3538) while escitalopram significantly decreased ASP^+ uptake (Dunn's test, 61.82 ± 0.70 a.u./μM^2 vs. 58.79 ± 0.47 a.u./μM^2, p = 0.0089). Fluoxetine + electrical stimulation did not significantly affect ASP^+ uptake (Dunn's test, 64.36 ± 0.94 a.u./μM^2 vs. 62.11 ± 0.58 a.u./μM^2, p = 0.3538). These data show that this phenomenon of increased ASP^+ reuptake is limited to escitalopram and not fluoxetine.

Figure 4I are voltammetric recordings in the cells 5 and 75 minutes after the administration of escitalopram at 3 different doses (0.1 µM, 0.5 µM and 1 µM). The average traces were fitted with the two-reuptake M-M equation shown above. **Figure 4J-L** shows the fitted ratio values with respect to the control state of $R(t)_{max}$, K_{m1} and V_{max1}, 5 and 75 minutes after the administration of escitalopram in the abovementioned doses. Interestingly, shortly after escitalopram (5 minutes) we see an increase in the rate of serotonin reuptake for 0.1 µM and 1 µM (0.1 µM: 3.60 nM s^{-1} *vs.* 5.22 nM s^{-1}; 1 µM: 3.00 nM s^{-1} *vs.* 3.32 nM s^{-1}) and no substantial effect for the 0.5 µM dose (2.90 nM s^{-1} *vs.* 2.57 nM s^{-1}). The reuptake rate slows progressively for all doses up to 75 minutes after this. These data provide clear chemical evidence that, as a result of escitalopram administration, serotonin can be reuptaken at a faster rate (depending on dose and time) due to increased SERT expression.

Having investigated the mechanisms of increased serotonin levels after SSRI and NRI administration *in vivo* and *in vitro*, we next explored why ketamine, a non-serotonin targeting drug, also increased ambient serotonin levels.

Histamine Mediates Ketamine's Effects on Ambient Serotonin

In this experimental paradigm, we administered ketamine (10 mg kg^{-1} *i.p.)* and monitored the changes in evoked histamine and serotonin dynamics over 100 min in the posterior hypothalamus (PH) of mice. **Figure 5A** shows representative examples of control histamine and serotonin color plots in the PH (top) and 40 min after administration of ketamine (bottom). Interpretation of these histamine/serotonin color plots can be found elsewhere in great detail(10). Briefly, evoked histamine release inhibits serotonin firing (*via* H3 receptors), the histamine and serotonin events are denoted in the color plot (**Fig. 5A**) and the concentration *vs.* time profiles (n = 5 animals, mean ± SEM) are shown in **Fig 5B.** Ketamine induced a rapid decrease in the maximum amplitude of histamine release (paired *t*-test, 8.92 ± 1.80 µM to 6.08 ± 1.61 µM, p = 0.0052). No significant effect on clearance rate was found 10 min after injection (paired t-test, 4.38 ± 1.27 s to 3.19 ± 0.97 s, p = 0.1686). Overall, we found significantly less inhibition of serotonin 10 min after drug injection (paired *t*-test, -44.70 ± 7.91 nM to -19.81 ± 4.97 µM, p = 0.0133). **Figure 5C** shows the average and SEM of the maximum amplitude of histamine (top) and serotonin inhibition amplitude (bottom) over time. The effects of ketamine are sustained 100 min after injection (paired *t*-test, HA: 8.92 ± 1.80 µM to 5.69 ± 0.94 µM, p = 0.0440; Ser.: paired *t*-test, -44.70 ± 7.91 nM to -26.66 ± 6.24 µM, p = 0.0065).

These data indicate that ketamine inhibits histamine release, serving to effectively reduce serotonin inhibition.

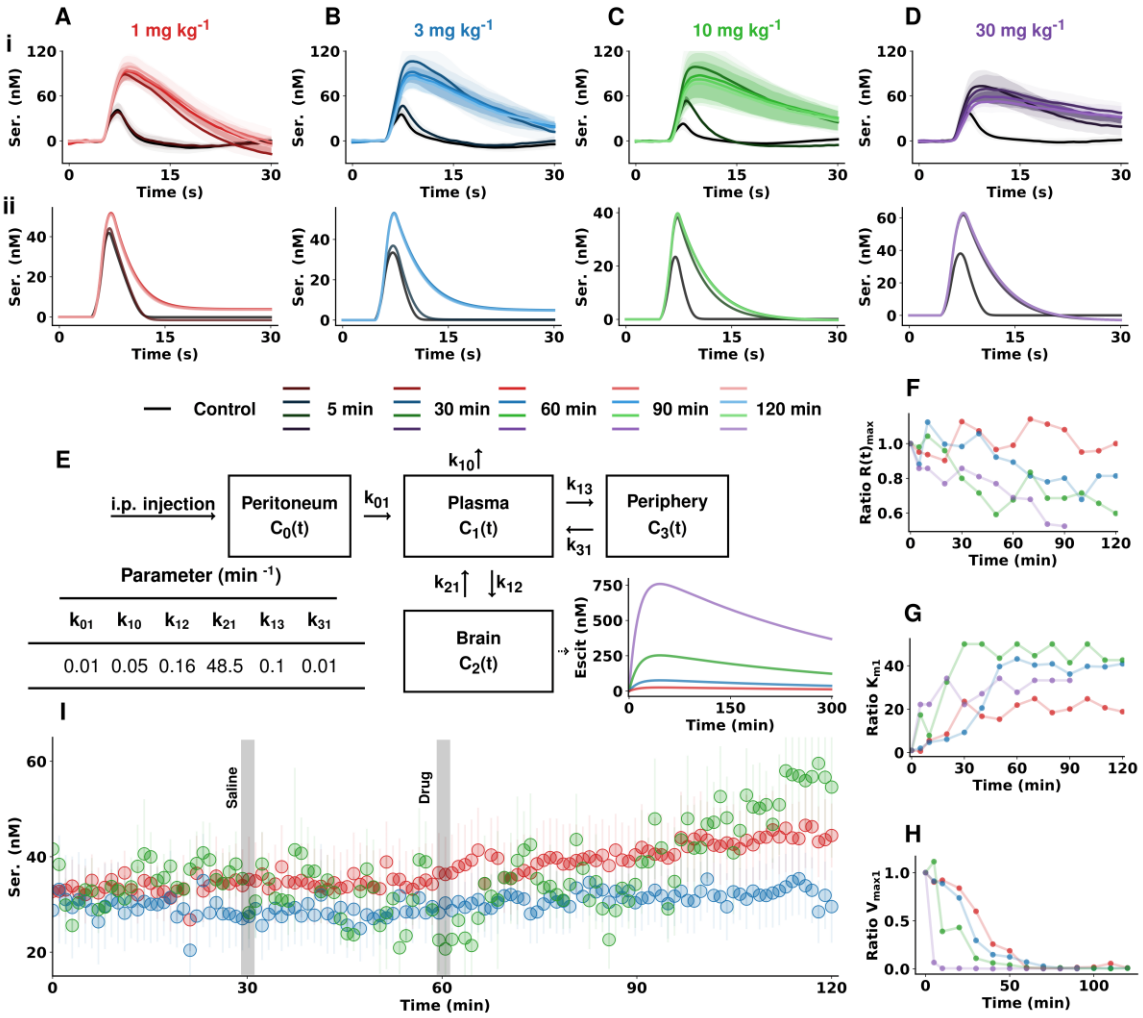

Figure S1. Escitalopram male data for (A) 1mg kg^{-1} (B) 3 mg kg^{-1} (C) 10 mg kg^{-1} (D) 30 mg kg^{-1}. (i) Evoked serotonin concentration vs. time traces from the CA2 region of the hippocampus of male mice before and after escitalopram administration (n = 4 animals each dose, mean ± SEM). (ii) Modeled serotonin concentration vs. time traces from the control data and after changing K_{m1} based on a simulated concentration of escitalopram in the brain with time according to the pharmacokinetic model depicted in (E) (see Methods section for a detailed description of the model). Compartment rate constants are obtained from literature of previous pharmacokinetic models of escitalopram in mice(5) (F-H) Modeled changes in maximum release rate of serotonin (F), K_{m1} (G) and V_{max1} (H) for each dose and over time after drug injection. (I) FSCAV recordings

of absolute concentrations of extracellular serotonin for 3 different doses of escitalopram (n = 5 animals for 1 mg kg^{-1} dose, n = 7 animals for 3 mg kg^{-1} and 10 mg kg^{-1} doses, mixed sex cohort).

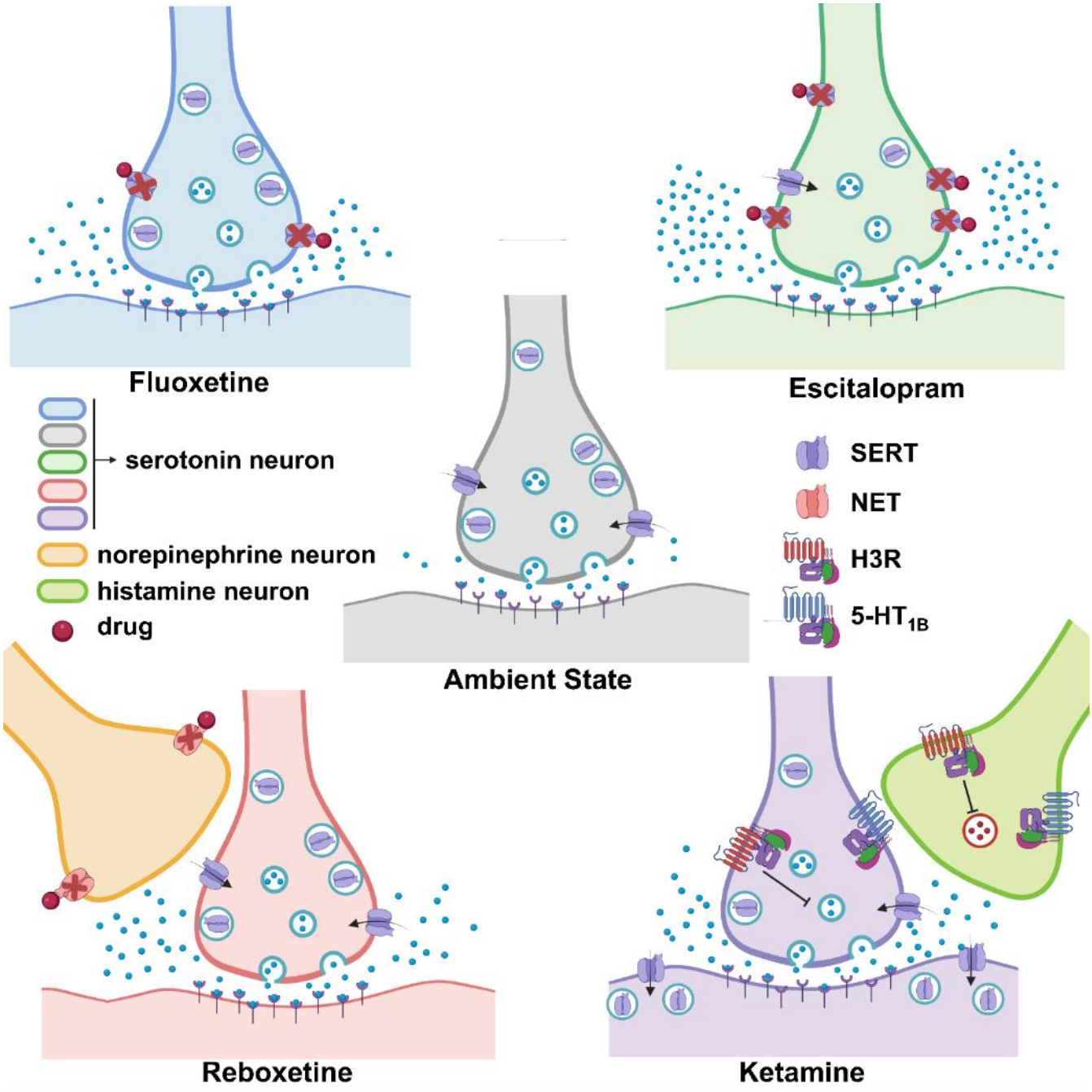

Figure S2. Mechanism of these antidepressant therapies on serotonin transmission. The ambient state exhibits normal serotonin signaling with uptake via SERTs. Fluoxetine orthosterically blocks SERTs to prolong serotonin in the synaptic space; serotonin is reuptaken *via* Uptake 2 transporters. Reboxetine blocks the NETs, so serotonin reuptake is mainly via SERTs. Ketamine acts on the serotonin via the histaminergic system. Ketamine inhibits histamine release, which subsequently disinhibits serotonin levels.

SI References

1. C. E. Witt *et al.*, Low-Frequency Oscillations of In Vivo Ambient Extracellular Brain Serotonin. *Cells* **11** (2022).
2. S. R. Jones, P. A. Garris, R. M. Wightman, Different effects of cocaine and nomifensine on dopamine uptake in the caudate-putamen and nucleus accumbens. *J Pharmacol Exp Ther* **274**, 396-403 (1995).
3. A. Baudry, S. Mouillet-Richard, B. Schneider, J. M. Launay, O. Kellermann, miR-16 targets the serotonin transporter: a new facet for adaptive responses to antidepressants. *Science* **329**, 1537-1541 (2010).
4. M. H. Buc-Caron, J. M. Launay, D. Lamblin, O. Kellermann, Serotonin uptake, storage, and synthesis in an immortalized committed cell line derived from mouse teratocarcinoma. *Proc Natl Acad Sci U S A* **87**, 1922-1926 (1990).
5. M. A. Bunin, C. Prioleau, R. B. Mailman, R. M. Wightman, Release and uptake rates of 5-hydroxytryptamine in the dorsal raphe and substantia nigra reticulata of the rat brain. *J Neurochem* **70**, 1077-1087 (1998).
6. N. Paul *et al.*, Activation of the glucocorticoid receptor rapidly triggers calcium-dependent serotonin release in vitro. *CNS Neurosci Ther* **27**, 753-764 (2021).
7. Allen (2015) Allen brain atlas api. (Allen Institute for brain science).
8. T. Lau, F. Heimann, D. Bartsch, P. Schloss, T. Weber, Nongenomic, glucocorticoid receptor-mediated regulation of serotonin transporter cell surface expression in embryonic stem cell derived serotonergic neurons. *Neurosci Lett* **554**, 115-120 (2013).
9. T. Lau, V. Proissl, J. Ziegler, P. Schloss, Visualization of neurotransmitter uptake and release in serotonergic neurons. *J Neurosci Methods* **241**, 10-17 (2015).
10. B. P. Jackson, S. M. Dietz, R. M. Wightman, Fast-scan cyclic voltammetry of 5-hydroxytryptamine. *Anal Chem* **67**, 1115-1120 (1995).
11. S. Samaranayake *et al.*, In vivo histamine voltammetry in the mouse premammillary nucleus. *Analyst* **140**, 3759-3765 (2015).
12. S. Mena *et al.*, Novel, User-Friendly Experimental and Analysis Strategies for Fast Voltammetry: Next Generation FSCAV with Artificial Neural Networks. *ACS Meas Sci Au* **2**, 241-250 (2022).
13. P. Hashemi, E. C. Dankoski, J. Petrovic, R. B. Keithley, R. M. Wightman, Voltammetric detection of 5-hydroxytryptamine release in the rat brain. *Anal Chem* **81**, 9462-9471 (2009).
14. S. Samaranayake *et al.*, A voltammetric and mathematical analysis of histaminergic modulation of serotonin in the mouse hypothalamus. *J Neurochem* **138**, 374-383 (2016).
15. A. Abdalla *et al.*, In Vivo Ambient Serotonin Measurements at Carbon-Fiber Microelectrodes. *Anal Chem* **89**, 9703-9711 (2017).
16. P. Welch, The use of fast Fourier transform for the estimation of power spectra: A method based on time averaging over short, modified periodograms. *IEEE Trans. Audo Electroacoust.* **15**, 70-73 (1967).
17. N. Rao, The clinical pharmacokinetics of escitalopram. *Clin Pharmacokinet* **46**, 281-290 (2007).
18. B. Sogaard, H. Mengel, N. Rao, F. Larsen, The pharmacokinetics of escitalopram after oral and intravenous administration of single and multiple doses to healthy subjects. *J Clin Pharmacol* **45**, 1400-1406 (2005).
19. A. Badea, A. A. Ali-Sharief, G. A. Johnson, Morphometric analysis of the C57BL/6J mouse brain. *Neuroimage* **37**, 683-693 (2007).
20. C. Bundgaard, M. Jorgensen, F. Larsen, Pharmacokinetic modelling of blood-brain barrier transport of escitalopram in rats. *Biopharm Drug Dispos* **28**, 349-360 (2007).
21. M. Kreilgaard, D. G. Smith, L. T. Brennum, C. Sanchez, Prediction of clinical response based on pharmacokinetic/pharmacodynamic models of 5-hydroxytryptamine reuptake inhibitors in mice. *Br J Pharmacol* **155**, 276-284 (2008).